X-660-76-25
PREPRINT

NASA TM X- 71077

ON THE ACCELERATION OF ENERGETIC PARTICLES IN THE INTERPLANETARY MEDIUM

L. A. FISK

JANUARY 1976

GSFC — GODDARD SPACE FLIGHT CENTER —
GREENBELT, MARYLAND

On the Acceleration of Energetic Particles in the Interplanetary Medium

L. A. Fisk *

Laboratory for High Energy Astrophysics

NASA/Goddard Space Flight Center

Greenbelt, Maryland 20811

* On leave at the Department of Physics, University of New Hampshire, Durham

ABSTRACT

Fermi-scattering and transit-time damping have been suggested as two possible mechanisms for accelerating low-energy protons ($\sim$1 Mev) in co-rotating particle streams. In this paper, the requirements and properties of each of these mechanisms are illustrated by means of numerical solutions to the equations which govern particle behavior in such streams. It is found that the conditions which are required for Fermi-scattering to be the dominant acceleration mechanism are more extreme than those required for transit-time damping. Acceleration by Fermi-scattering requires a scattering mean-free path more than an order of magnitude smaller than the nominal value for low-energy particles of 0.1 AU. Transit-time damping of only the observed low-level of magnitude fluctuations in the interplanetary magnetic field appears to yield the required acceleration rate. Measurements of the direction of the anisotropy in the particle streams could be of help in deciding which of these mechanisms (if either) is operative. In the case of Fermi-scattering the anisotropy must be in the heliocentric radial direction, whereas for transit-time damping a significant azimuthal anisotropy could be present.

McDonald et al. (1976), by comparing Pioneer 11 and IMP-7 data, have found recently that the intensity of 1-Mev protons in co-rotating streams increases by more than an order of magnitude between 1 and 3 AU from the sun. Although other interpretations of these data may be possible, McDonald et al. (1976) draw the reasonable conclusion that these observations are compelling evidence for extensive interplanetary acceleration of low-energy particles. McDonald et al. (1976) suggest that a possible mechanism for this acceleration is a Fermi - scattering process, as has been discussed by, for example, Jokipii (1971) and Wibberentz and Beuermann (1972). In this mechanism particles are statistically accelerated by interacting with randomly propagating Alfven waves which have wave lengths comparable in size to the particle gyro-radii. Equivalently, the particles are accelerated by cyclotron damping of the Alfven waves. Fisk (1976a) has suggested that an alternative mechanism is transit-time damping. In this process particles are statistically accelerated by interacting with fluctuations in the magnitude of the interplanetary magnetic field (e.g. magnetosonic waves). By using only the low-level of magnitude fluctuations that are observed in the inner solar system, Fisk (1976a) finds an acceleration rate which appears to be sufficient to account for the intensity increases reported by McDonald et al. (1976). It is the purpose of the present paper to illustrate the requirements and properties of each of these possible acceleration mechanisms by

means of numerical solutions to the equations which describe particle behavior in steady-state co-rotating streams.

The discussion here is limited to acceleration by Fermi-scattering and by transit-time damping. The exclusion of other acceleration mechanisms should not be construed, however, as implying that Fermi-scattering and transit-time damping are the only possibilities. For example, some of the observed intensity increases could result from acceleration of particles by interplanetary shock waves.

The Model

It is assumed here that protons are injected into co-rotating streams at heliocentric radial distances that are small compared with 1 AU, and at energies small compared with the observed energies of $\gtrsim$100 keV. For example, the protons could originate in the suprathermal tail of the solar wind near the sun. The protons are then assumed to be accelerated in a statistical process, or, equivalently, to diffuse in momentum space. This acceleration competes against the normal adiabatic deceleration which results from the expansion of the solar wind (Parker, 1965). The protons also diffuse spatially and are convected by the solar wind. It is expected that this simple model will illustrate many of the features of particle acceleration in co-rotating streams. It should be recognized, however, that particle behavior could be different in some details in models where the injection occurs continuously with radial distance (e.g. where particles are continuously accelerated out of the solar wind), or in models where particles are injected at the sun with energies comparable to the observed energies.

It is also assumed here that the solar wind flows in the radial direction with constant speed V. The mean interplanetary magnetic field, as a result, executes a simple Archimedes spiral pattern. A mean field line, or flux tube, then lies along a curve of constant ϕ^*, where (Parker, 1963; Ng, 1972)

$$\phi^* = \phi - \Omega t + \Omega(r-r_s)/V \qquad (1)$$

Here, ϕ is the azimuthal angle in a spherical coordinant

system which has a polar axis along the axis of rotation of the sun. The angular velocity of the sun is Ω; t is time; r is heliocentric radial distance; and r_s is the radius of the sun. Clearly ϕ^* marks the location of the footpoint of the mean field line at the surface of the sun, at t = 0.

It is further assumed here that particles propagate only along the mean field direction, i.e. cross-field diffusion is ignored. As discussed in detail in Ng (1972), the behavior of particles in one flux tube is then independent of the behavior in other flux tubes. A convenient coordinant system to choose is thus r and ϕ^*, as opposed to r and ϕ, since the particle behavior at different values of ϕ^* is now unrelated.

The equation for the omni-directional distribution function f (particles per unit volume of phase space, averaged over particle direction) in a steady-state co-rotating stream can be written in terms of r and ϕ^* as (Parker, 1965; Gleeson and Axford, 1969; Ng, 1972; Fisk et al., 1973; Fisk, 1976a)

$$-\frac{2V}{3r}p\frac{\partial f}{\partial p} = \frac{1}{r^2}\frac{\partial}{\partial r}(r^2\kappa_{\shortparallel}\cos^2\psi\frac{\partial f}{\partial r}) + \frac{1}{p^2}\frac{\partial}{\partial p}(p^2\bar{D}_{pp}\frac{\partial f}{\partial p}) - V\frac{\partial f}{\partial r} \qquad (2)$$

This equation determines f as a function of radial distance r and particle momentum p, within a given flux tube or stream, i.e. along curves of constant ϕ^*. Particle differential intensity j per unit interval of kinetic energy T, is related to f by $j = f/p^2$.

The first term on the right side of (2) describes the

diffusion of particles in the heliocentric radial direction, where $\kappa_{\parallel}$ is the diffusion coefficient for propagation along the mean magnetic field, and where ψ is the angle between the mean field and the radial direction. The second term on the right of (2) describes the diffusion of particles in momentum space, i.e. it describes the statistic acceleration. Here $\bar{D}_{pp}$ (in the notation of Fisk (1976a)) is the rms change in momentum per unit time averaged over particle direction. The third term on the right of (2), and the term on the left side, describe the convection and adiabatic deceleration of particles in the expanding solar wind.

Equation (2) can also be written in terms of the differential number density U, per unit interval of kinetic energy T, or as

$$\frac{1}{r^2}\frac{\partial}{\partial r}(r^2\kappa_{\parallel}\cos^2\psi\frac{\partial U}{\partial r}) + \frac{\partial}{\partial T}(D_{TT}\frac{\partial U}{\partial T}) - \frac{\partial}{\partial T}(\frac{D_{TT}}{2T}U)$$

$$+ \frac{2V}{3r}\frac{\partial}{\partial T}(\alpha TU) - \frac{V}{r^2}\frac{\partial}{\partial r}(r^2U) = 0 \qquad (3)$$

Here, $D_{TT} = v^2\bar{D}_{pp}$, where v is particle speed; $\alpha = (T+2T_o)/(T+T_o)$, with T_o particle rest energy. The statistical acceleration results in an rms change in energy, which is described by the coefficient D_{TT}, and in a mean energy change, which is given by the term $D_{TT}/2T$. In the analysis of Jokipii (1971) and McDonald et al. (1976) only the mean energy change is considered. In many cases, however, including the ones discussed here, the rms change

Illustrative Examples

Equation (2) or (3) can be solved numerically by using the technique that is outlined in the appendix to this paper. Consider now two examples of these solutions, which illustrate the requirements and properties of (i) a Fermi-scattering mechanism and (ii) transit-time damping as a means for explaining the observations of McDonald et al. (1976). In both examples the parameters are chosen so that the calculated intensity has the reasonable value of $j = 1$ proton/cm^2-sec-ster-Mev at $r = 1$ AU and $T = 1$ Mev. It is further required that the calculated intensity increases by a factor $\sim$10 between $r = 1$ and 3 AU.

(i) Fermi-scattering

Jokipii (1971) reports that the mean change in energy that results from acceleration by a Fermi-scattering process is

$$\frac{dT}{dt} = \frac{D_{TT}}{2T} \simeq \frac{8V_A^2 T}{3\kappa_{\mu}} \qquad (4)$$

where V_A is the Alfven speed. However, as can be seen from the work of Wibberentz and Beuermann (1972), this expression for the acceleration rate is too large by roughly a factor of 5. The assumption made by Jokipii (1971) that particle pitch angle can be ignored in the derivation of (4) is unfounded since dT/dt varies roughly as pitch angle cubed.

In the calculations presented here D_{TT} for acceleration by Fermi-scattering is taken to be

$$D_{TT} \simeq \frac{V_A^2 T^2}{\kappa_{\mu}} \qquad (5)$$

The Alfven speed is taken to be V_A = 50 km/sec. The parallel diffusion coefficient is assumed to have the simple form $\kappa_{\parallel} = 1/3\ v\lambda$ where λ is a constant independent of position and particle rigidity. The magnitude of $\kappa_{\parallel}$ is taken to be such that $\kappa_{\parallel} \simeq 1.8 \cdot 10^{19}$ cm^{2}sec^{-1} at T = 1 Mev. The rms change in energy, per unit time, is then

$$D_{TT} \simeq 1.4 \cdot 10^{-6} T^{3/2} \text{ (Mev}^2\text{/sec)} \qquad (6)$$

where T is in units of Mev.

The solar wind speed is taken here to be V = 400 km/sec and the Archimedes spiral pattern of the mean field is normalized so that $\cos^2\psi = 0.5$ at r = 1 AU. The number of particles per unit time and solid angle, which are injected into the co-rotating stream, is taken to be $Q = 2.8 \cdot 10^{27}$ protons/sec-ster.

With these parameters, and with the injection procedure specified in the previous section, the intensity determined by (3) has been calculated as a function of energy for various radial distances. The results are shown in Figure 1a. As can be seen in this figure, the parameters chosen here yield the required factor $\sim$10 increase in the 1 Mev intensity between 1 and 3 AU, as well as the required intensity of j = 1 proton/cm^2-sec-ster-Mev at r = 1 AU and T = 1 Mev.

It should be noted that with the specification of V_A, $\kappa_{\parallel}$ in this example determines both the acceleration and the spatial diffusion of the particles. Accordingly, the

requirement that the intensity at 1 Mev increases by a factor of $\sim$10 between 1 and 3 AU essentially uniquely determines κ_{μ} at this energy.

It should be emphasized here also that the magnitude of κ_{μ} that is required to produce the observed factor of $\sim$10 increase is exceedingly small. For example, this κ_{μ} yields a mean free path for a 1-Mev proton of only $\lambda \sim 3 \cdot 10^{-3}$AU, which is only $\sim$15 times the particle gyro-radius in a typical interplanetary magnetic field of $5 \cdot 10^{-5}$ Gauss. This value for λ is much smaller than the nominal mean free path for low-energy particles of $\lambda \sim 0.1$ AU (Ma Sung et al., 1975).

(ii) Transit-time damping

As can be seen in the discussion in Fisk (1976a), the transit-time damping acceleration rate is unrelated to the pitch-angle scattering rate. Particles are accelerated in this mechanism by interacting with long-wavelength magnetosonic waves, an interaction which conserves the particles' magnetic moment. The pitch-angle scattering results from interactions with Alfven waves which have scale-sizes comparable to the particle gyro-radii. The diffusion coefficient κ_{μ} can thus in this case be chosen independent of D_{TT}. In the calculations here κ_{μ} is again assumed to be independent of particle rigidity. The magnitude of κ_{μ}, however, is now taken to be such that $\kappa_{\mu} = 7 \cdot 10^{20} cm^2 sec^{-1}$ at T = 1 Mev, which is the magnitude that results with the mean free path taken to be the nominal value of λ = 0.1 AU. Further, κ_{μ} is assumed to increase with heliocentric distance

in such a manner that $\kappa_{\parallel}\cos^2\psi$ remains constant.

For the acceleration rate for transit-time damping it was shown in Fisk (1976a) that

$$\frac{\bar{D}_{pp}}{p^2} = 1.2\cdot 10^{-7} T^{-\frac{1}{2}} (\text{sec}^{-1}) \tag{7}$$

which corresponds to

$$D_{TT} = 5\cdot 10^{-7} T (\text{Mev}^2/\text{sec}) \tag{8}$$

where T in both (7) and (8) is measured in units of Mev. The formulae on which this acceleration rate is based are calculated by using standard quasi-linear/adiabatic theory. The acceleration rate is evaluated by using parameters that should describe the low level of small-scale fluctuations in the magnitude of magnetic field which are observed in the inner solar system. For example, the amplitude of the fluctuations δB, relative to the mean field strength B_o, is taken to be $(\delta B/B_o)^2 \approx 0.01$, in agreement with the observations of, e.g., Smith (1974).

The solar wind speed is again V=400 km/sec and $\cos^2\psi$=0.5 at r=1 AU. The number of particles that are injected into the co-rotating stream is $Q=7\cdot 10^{27}$ protons/sec-ster.

With these parameters and with the injection procedure specified in the previous section, the intensity spectrum at various radial distances have been calculated from the numerical solution to (3). The results are shown in

Figure 1b. Again, the parameters chosen here yield the required intensity at r=1 AU and T=1 Mev, as well as the required increase in the 1-Mev intensity between 1 and 3 AU.

It should be noted that the number of particles that must be accelerated in both of these examples is quite small ($Q \approx 5 \cdot 10^{27}$protons/sec-ster). Suppose, for example, that the accelerating region has an inner boundary at r_o=0.1 AU, and particles are injected into this region by being convected in at the solar wind speed. The number density of injected particles is then only $n \approx Q/(r_o^2 V) \approx 5 \cdot 10^{-5}$protons/cm^3.

The number of particles which are accelerated to energies of, e.g., 1 Mev is quite sensitive to the acceleration rate. As can be seen in the approximate solution to (3) which is given in the appendix, the number accelerated varies as the exponential of $-VT^2/(D_{TT}r)$. It is thus interesting to note that with a similar number of particles injected, transit-time damping requires a noticeably smaller acceleration rate than does Fermi-scattering to produce the same flux at r=1 AU and T=1 Mev. At T=1 Mev, D_{TT} in (8) is roughly a factor of 3 smaller than D_{TT} in (6). In the model considered here particles are injected into the co-rotating stream at some small radial distance and then accelerated as they propagate to 1 AU. In the case of Fermi-scattering, κ_{μ} is sufficiently small so that particles move essentially only by being convected by the solar wind. The available time in which to accelerate the particles seen near earth is then only the transit time of the solar wind to 1 AU.

In transit-time damping, however, the particles are more mobile. Particles, for example, could be convected out to a distance of several AU and then diffuse back to near earth. The time that is available in which to perform the acceleration is thus longer with transit-time damping, or equivalently, the required acceleration rate is less.

In both of the examples given here the intensity at $\sim$1 Mev reaches a maximum at several AU from the sun, and then decrease with increasing r. This decrease occurs even though the acceleration rate is constant as a function of r. Particles are injected only at small radial distances and low energies. As the particles propagate away from the injection point and are accelerated to higher energies, the number of particles left at lower energies thus diminishes, or equivalently, the intensity here decreases. In interpreting observations, then, a decrease with increasing r in the intensity at a given energy should not, by itself, be taken as evidence that the acceleration is diminishing. Such a decrease in the acceleration rate can be inferred only if it can be shown that the intensity at higher energies is also declining.

It is noted finally that the spectral shapes that result in both of the numerical examples considered here exhibit, in a crude sense, some of the features found in the observed spectra. McDonald et al. (1976) report that at energies above $\sim$400 keV the observed spectra can be fit with an exponential: $\exp(-T/T')$, where $T' \sim 1$ Mev. At

energies below ∿400 keV, however, the observed spectra do not flatten as would be expected from an exponential, but rather rise toward the lower energies. The dashed curve in Figure 1a is an exponential with T'∿800 keV. As can be seen in this figure, the calculated spectrum at r=2 AU is reasonably well fit by this exponential at energies above ∿1 Mev, and produces some excess over the exponential below this energy. The spectra shown in Figure 1b also exhibit this behavior. These latter spectra, however, are fit at energies ≳1 Mev with a steeper exponential, i.e. T'∿300 keV.

The spectral shapes shown in Figures 1a and 1b are, however, model-dependent. In circumstances other than the ones used in these examples, the spectral shapes could be different. For example, if $\kappa_{\parallel}$ in the Fermi-scattering case were proportional to particle rigidity as well as velocity, the acceleration rate D_{TT}/T^2 would vary as T^{-1}, rather than as $T^{-1/2}$ as in (6). This more rapid decrease in the acceleration rate results in steeper spectra at the higher energies; in fact, the resulting spectra are similar in shape to the spectra in the transit-time damping example. Further, if particles are injected continuously with radial distance, the calculated spectra may not turn over at low energies (as in Figures 1a and 1b), but rather, in this range, may have a steep negative slope.

Concluding Remarks

The conditions that are required for Fermi-scattering to be the dominant mechanism for accelerating particles in co-rotating streams appear to be more extreme than those required for transit-time damping. Based on the calculations in Fisk (1976a), it appears that transit-time damping of the observed small-scale fluctuations in the magnitude of the interplanetary field yields an acceleration rate that is sufficient to account for the observations of McDonald et al. (1976). A similar acceleration rate by the Fermi-scattering mechanism requires a mean-free path that is more than an order of magnitude smaller than the nominal value of 0.1 AU. It is therefore tempting to conclude that transit-time damping is the more likely of the two acceleration mechanisms.

This conclusion, however, should be made only with some caution. As is pointed out by McDonald et al. (1976), the observed co-rotating particle streams coincide with stream-stream interaction regions in the solar wind. The enhanced turbulence in these regions could conceivably result in the small mean-free path required for Fermi-scattering. Moreover, it is assumed in the transit-time damping calculations of Fisk (1976a) that the observed magnitude fluctuations are the result of fast-mode magnetosonic waves. If some of the magnitude fluctuations are due to other modes (e.g. they could be due in part to static structures in the field), the acceleration rate by transit-time damping will be reduced.

Of course, with detailed observations of co-rotating

streams, it may be possible to decide which of these mechanisms, if either, is in fact operative. As is discussed above, the spectral shapes predicted by both the Fermi-scattering and the transit-time damping mechanisms can be similar and, in any case, the spectra are model-dependent. Measurements of the intensity alone are, therefore, not expected to be very revealing. A somewhat better observational test for deciding between these two mechanisms may come instead from measurements of the direction of the anisotropy in the streams.

In a co-rotating stream the radial anisotropy is given by Ng (1972):

$$\xi_r = \frac{3}{v}\left(CV - \frac{\kappa_{\parallel}\cos^2\psi}{U}\frac{\partial U}{\partial r}\right) \tag{9}$$

where

$$C = 1 - \frac{1}{3U}\frac{\partial}{\partial T}(\alpha T U) = -\frac{\partial \ell n f}{\partial \ell n p} \tag{10}$$

is the Compton-Getting coefficient. The azimuthal anisotropy is

$$\xi_\phi = \frac{3\kappa_{\parallel}\cos\psi\sin\psi}{vU}\frac{\partial U}{\partial r} \tag{11}$$

The anisotropy makes an angle $\chi \equiv \tan^{-1}(\xi_\phi/\xi_r)$ with the heliocentric radial direction.

In the case of Fermi-scattering, the required $\kappa_{\parallel}$ is sufficiently small so that $\xi_r \simeq 3CV/v$ and $|\xi_\phi| << |\xi_r|$. The anisotropy vector in this case is then closely aligned with the radial direction. For example, in the above numerical solution, which illustrates the requirements of the Fermi-scattering mechanism, $|\chi| < 1°$. The magnitude of the anisotropy

in the example is ∿40% near r=1 AU, where the spectrum is steep, and it declines to ∿10% at r=4 AU.

In the case of transit-time damping, however, $\kappa_{\parallel}$ can be sufficiently large so that a detectable azimuthal anisotropy is present. Plotted in Figure 3, as a function of r, are values of χ and ξ_ϕ that are calculated from the above numerical solution which illustrates the requirements of transit-time damping. In addition to noting in this figure that ξ_ϕ is sufficiently large to be detectable, it is interesting to note that ξ_ϕ changes sign as r increases. As can be seen from (11), this sign change occurs where the radial gradient $(\partial U/\partial r)$ changes sign.

Clearly, if the anisotropy is found to lie in other than the radial direction in co-rotating streams, acceleration by Fermi-scattering can be eliminated as a viable acceleration mechanism. Detection of an appreciable azimuthal component would be consistent with acceleration by transit-time damping. However, such an observation is not proof that the acceleration occurs in this manner since other acceleration mechanisms are still possible. Conversely, detection of a strictly radial anisotropy would suggest that the particles are experiencing extensive scattering, sufficient perhaps to accelerate by a Fermi-scattering mechanism. However, this observation does not eliminate the transit-time damping mechanism since this acceleration could also be performed in the presence of considerable scattering.

Acknowledgments

The author has enjoyed many stimulating discussions with Drs. F. B. McDonald, B. J. Teegarden, and T. T. Von Rosenvinge, who have kindly revealed unpublished details of particle behavior in co-rotating streams.

APPENDIX

Equations (2) and (3) are elliptical partial differential equations, and as such must be solved numerically by an iterative procedure. The appropriate technique is to add a term $A(r,T)\partial U/\partial t$ to, for example, (3), which then becomes

$$\frac{1}{r^2}\frac{\partial}{\partial r}(r^2\kappa_{\parallel}\cos^2\psi\frac{\partial U}{\partial r}) + \frac{\partial}{\partial T}(D_{TT}\frac{\partial U}{\partial T}) - \frac{\partial}{\partial T}(\frac{D_{TT}}{2T}U)$$

$$+ \frac{2V}{3r}\frac{\partial}{\partial T}(\alpha TU) - \frac{V}{r^2}\frac{\partial}{\partial r}(r^2U) = A(r,T)\frac{\partial U}{\partial t} \qquad (A.1)$$

where t is time and $A(r,T)$ is a function of r and T, which will be specified. By starting from an initial condition $U(r,T,t)$ at $t=0$, and with appropriate boundary conditions, (A.1) is then used to generate the solution $U(r,T,t)$ at subsequent times. The procedure is continued until such time that $\partial U/\partial t \to 0$, i.e. until the solution relaxes to the required steady-state solution.

To obtain a numerical solution, (A.1) is of course converted into a series of finite difference equations which determine the solution at various grid points. Thus, $U(I,J,K)$ is determined where $r=\Delta r\cdot I+r_{min}$; $T=\Delta T\cdot J+T_{min}$; $t=\Delta t\cdot K$; Δr, ΔT, and Δt are the constant spacing between the grid points, and r_{min} and T_{min} are, respectively, the minimum values of r and T. It is also convenient, in some instances, to change variables in (A.1) from r and T to ℓnr and ℓnT. The grid points then are spaced such that $\ell nr = \Delta\ell nr\cdot I+\ell nr_o$, and $\ell nT = \Delta\ell nT\cdot J+\ell nT_o$, where $\Delta\ell nr$ and $\Delta\ell nT$ are constant. With these latter variables, the solution

can be determined over a wide range of energies and radial distances. Also, by using ℓnr as the variable, there are many grid points at small r, where the solutions frequently vary strongly.

The form of (A.1) is similar to the form of the equation which governs solar modulation in models where interplanetary conditions vary with heliocentric latitude, θ. The variables r, T and t in (A.1) are, respectively, the analogues of the variables r, θ, and particle momentum p in the modulation problem. The technique which is outlined in Fisk (1976b) for solving the modulation equation can thus be applied directly to the solution of the finite difference equations that result from (A.1).

It might seem on physical grounds that A(r,T) should be set equal to unity, since then (A.1) is simply the time-dependent form of (3) (cf. Gleeson and Axford, 1967). For example, with A≡1, (A.1) could be used to describe the evolution of a stream with a time-varying source. In practice, however, this choice for A is inappropriate. Rather, to achieve a numerically-stable solution, A must be chosen so that the solution converges from the initial condition U(r,T,0) to the steady-state solution at roughly the same rate at all values of r and T. An appropriate choice for A has been found by trial and error to be

$$A(r,T) = B\left|\frac{\kappa_{rr}\cos^2\psi}{(\Delta r)^2} + \frac{D_{TT}}{(\Delta T)^2}\right|\Delta t \qquad (A.2)$$

where B is a number ~ 0.1. With this choice, the effective time-step at each grid point is roughly the time required for

particles to diffuse, in space or in energy, to the grid point from several grid points away. In cases where (A.1) is written in terms of ℓnr and ℓnT, Δr and ΔT in (A.2) should be replaced by $r(\Delta \ell nr)$ and $T(\Delta \ell nT)$, respectively.

For the initial condition $U(r,T,0)$, an approximate solution to (3) can be used. As is discussed in Fisk (1976a) (2) can be solved analytically in the limit where the spatial diffusion term (the first term on the right of (2)) can be neglected. In particular, solutions are available for the conditions used in the examples given in the present paper, i.e. when $\bar{D}_{pp}=D_o p^{\beta}$, with D_o and β constants, and when the injection occurs at low momenta and small radial distances. In terms of U, this approximate solution is

$$U(r,T) = \frac{2\pi T^{1/2} Q}{V(4-2\beta')^{(1+\beta')/(2-\beta')}} \frac{r^{-\left(\frac{11-4\beta'}{4-2\beta'}\right)}}{\Gamma[3/(4-2\beta')]}$$

$$\cdot \left(\frac{4(11-4\beta')V}{3D_o'}\right)^{\frac{3}{4-2\beta'}} \exp\left|-\frac{(11-4\beta')}{3(2-\beta')^2}\frac{T^{2-\beta'}V}{D_o' r}\right| \qquad (A.3)$$

where $D_{TT}=D_o' T^{\beta'}$ (D_o and β' are constants), and $\Gamma(z)$ is the gamma function. Again, Q is the number of particles injected per unit time and solid angle. The effects of spatial diffusion tend to be small at low energies, particularly for acceleration by Fermi-scattering. This approximate solution thus tends to be a reasonable approximation to the exact numerical solution. Equivalently, the number of iterations that is required to obtain the exact solution is not large.

For one of the boundary conditions, U(r,T,t) is taken to be zero at the maximum value of r, i.e. the interplanetary medium is assumed to have a free escape boundary. For the two examples given here, the boundary is placed at approximately r=20 AU. Also, few particles are assumed to obtain high energies, i.e. U(r,T,t) is set equal to zero at the maximum energy considered, which is taken here to be 20-30 Mev. Since (A.3) becomes an excellent approximation to the exact solution at very low energies, U(r,T,t) is set equal to (A.3) at the minimum energy T_{min}, which is taken to be T_{min}=10 keV. Finally, it is required that $\partial U/\partial r=0$ at $r=r_{min}$, which is placed at r=0.2 AU. Strictly speaking, this last boundary condition is incompatible with the initial condition (A.3). However, as is frequently the case in these problems, the boundary condition at small r has little effect on the solution near earth and beyond. It is sufficient, as is done here, simply to choose a boundary condition which is easy to implement numerically.

REFERENCES

Fisk, L. A., The acceleration of energetic particles in the interplanetary medium by transit-time damping, submitted to J. Geophys. Res., 1976a.

Fisk, L. A., Solar modulation of galactic cosmic rays 4. Latitude-dependent modulation, submitted to J. Geophys. Res., 1976b.

Fisk, L. A., M. A. Forman, and W. I. Axford, Solar modulation of galactic cosmic rays 3. Implications of the Compton-Getting coefficient, J. Geophys. Res., 78, 995, 1973.

Gleeson, L. J. and W. I. Axford, Cosmic rays in the interplanetary medium, Astrophys. J., 149, L115, 1967.

Jokipii, J. R., Deceleration and acceleration of cosmic rays in the solar wind, Phys. Rev. Letters, 26, 666, 1971.

MaSung, L. S., VanHollebeke, M. A., and McDonald, F. B., Propagation characteristics of solar flare particles, Conf. Papers, 14th Inter. Conf. Cosmic Rays, Munich, 5, 1767, 1975.

McDonald, F. B., B. J. Teegarden, J. H. Trainor, T. T. von Rosenvinge, and W. R. Webber, The interplanetary acceleration of energetic nucleons, Astrophys. J. (Letters), in press, 1976.

Ng, C. K., Propagation of solar-flare cosmic rays, Ph.D. thesis, Monash U., 1972.

Parker, E. N., Interplanetary Dynamical Processes, Interscience, New York, 1963.

Parker, E. N., The passage of energetic charged particles through interplanetary space, Planet. Space Sci., 13, 9, 1965.

Smith, E. J., Radial gradients in the interplanetary magnetic field between 1.0 and 4.3 AU: Pioneer 10, Solar Wind Three, ed. by C. T. Russell, published by IGPP, U. of Calif., Los Angeles, p. 257, 1974.

Wibberenz, G., and Beuermann, Fermi acceleration in interplanetary space, Cosmic Plasma Physics, ed. by K. Schindler, Plenum Press, New York, 339, 1972.

FIGURE CAPTIONS

Figure 1 A plot vs. kinetic energy of the calculated intensities in a co-rotating stream, at various radial distances. The intensity spectra in the right figure (1a) result from acceleration by a Fermi-scattering mechanism; the intensity spectra in (1b), from a transit-time damping mechanism. The dashed curve is given by an exponential: $\exp(-T/T')$, with $T' = 800$ keV.

Figure 2 The direction of the anisotropy (χ) and the magnitude of the azimuthal anisotropy (ξ_ϕ) in a co-rotating stream, where the acceleration is by transit-time damping. The curves are plotted here as a function of heliocentric radial distance at two energies: 1 Mev and 500 keV. The parameters used in calculating χ and ξ_ϕ are the same as those used in calculating the intensities in Figure 1b. The angle χ is measured relative to the heliocentric radial direction.

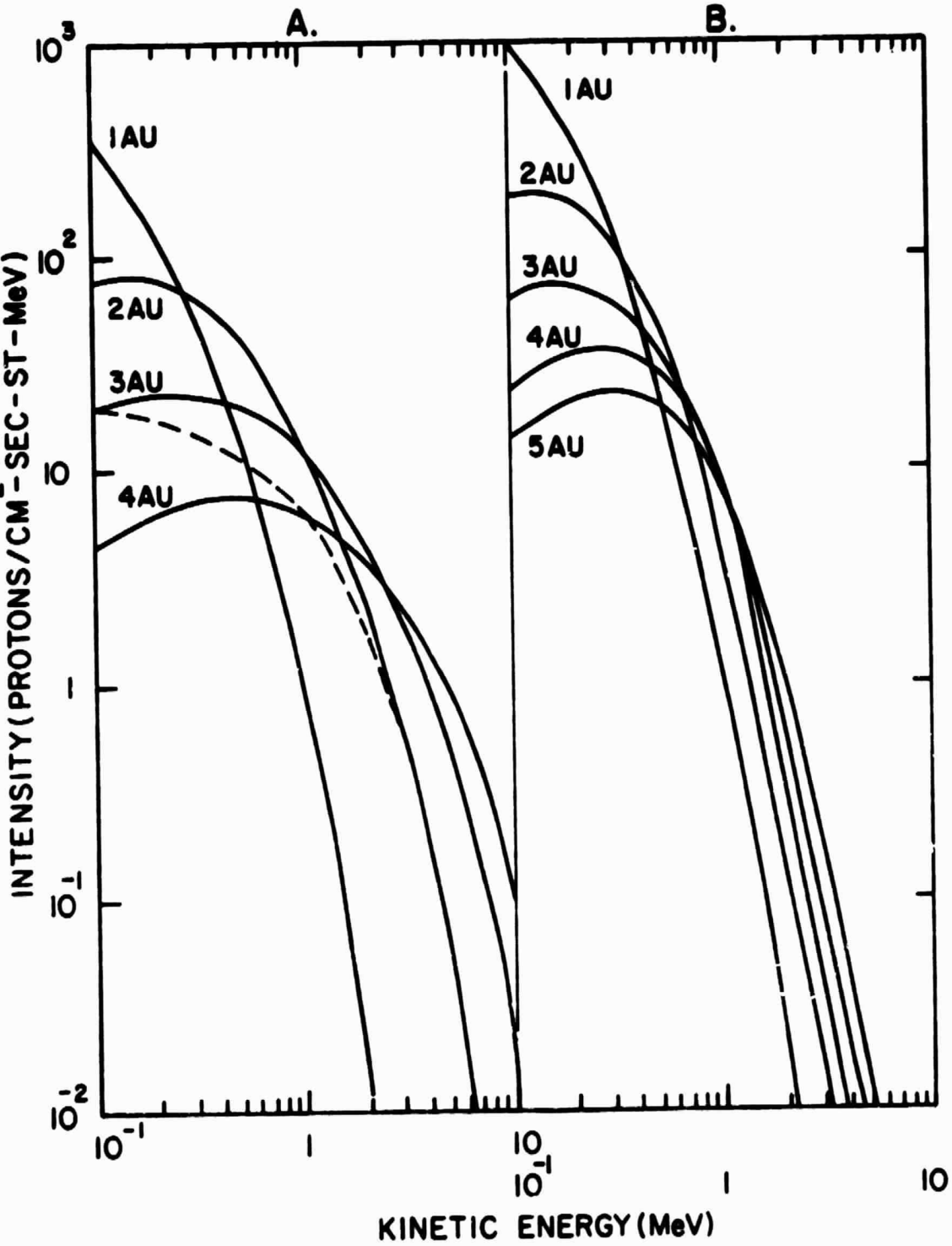
A.
B.
1AU
2AU
3AU
4AU
5AU
INTENSITY (PROTONS/CM²-SEC-ST-MeV)
KINETIC ENERGY (MeV)

FIGURE 1

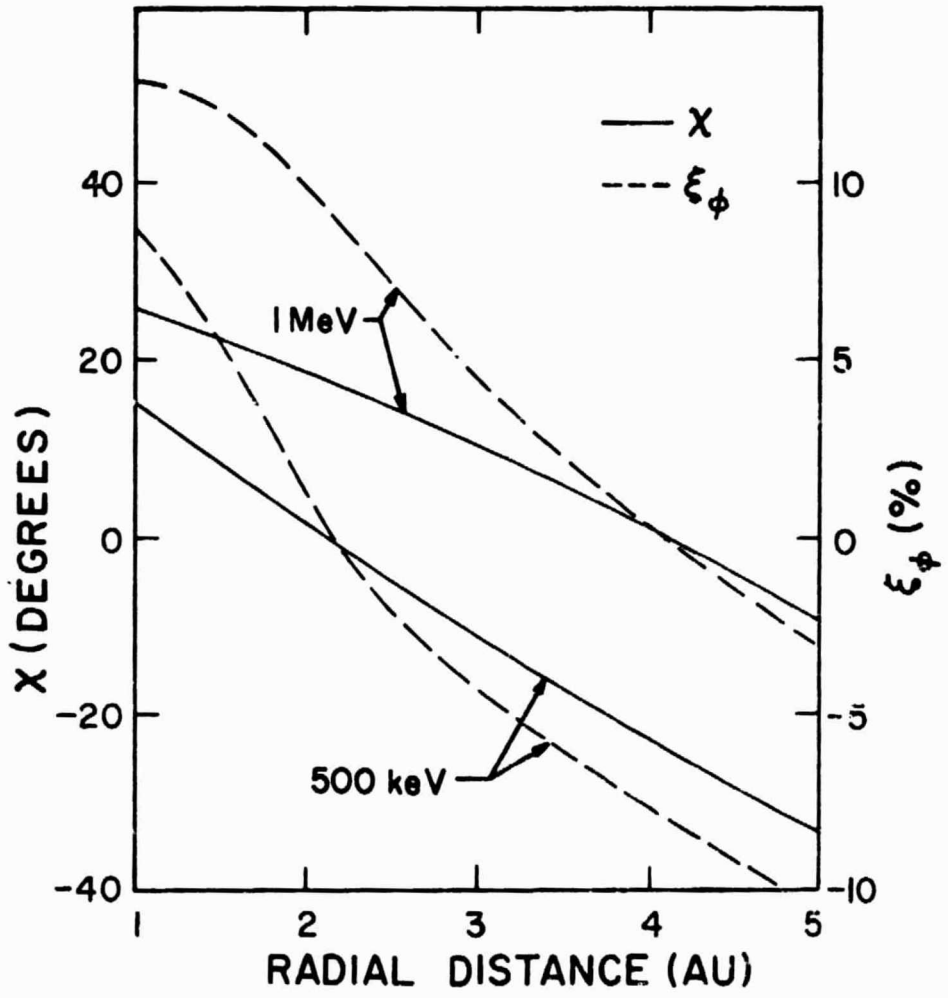

FIGURE 2

PREPRINT